

1 **Immune checkpoint inhibitor treatment does not impair ovarian or endocrine function in**
2 **a mouse model of triple negative breast cancer**

3
4
5

6 **Payton De La Cruz^{1,2}, Morgan F. Woodman-Sousa^{2,3}, Julia N. McAdams², Ellia Sweeney⁴,**
7 **Lola Hakim⁴, Melanie Morales Aquino⁴, Kathryn J. Grive^{2,5}**

8
9
10

- 11 1. Brown University, Pathobiology Graduate Program, Providence, RI, 02906
- 12 2. Women and Infants Hospital of Rhode Island, Department of Obstetrics and Gynecology,
13 Program in Women's Oncology, Providence, RI 02905
- 14 3. Brown University, Molecular Biology, Cell Biology, and Biochemistry Graduate Program,
15 Providence, RI, 02906
- 16 4. Brown University, Division of Biology and Medicine, Providence, RI, 02906
- 17 5. Warren Alpert Medical School of Brown University, Department of Obstetrics and Gynecology,
18 Providence, RI 02905

19
20
21
22

23 *Corresponding author:* EMAIL kgrive@wihri.org; PHONE (401)-274-1122 ext: 48031

24

25 *Permanent address:* Kilguss Research Institute, 200 Chestnut St., Room 108, Providence, RI
26 02903, USA

27 **ABSTRACT**

28 *Background:* Representing 15-20% of all breast cancer cases, triple negative breast cancer
29 (TNBC) is diagnosed more frequently in reproductive-age women and exhibits higher rates of
30 disease metastasis and recurrence when compared with other subtypes. Few targeted treatments
31 exist for TNBC, and many patients experience infertility and endocrine disruption as a result of
32 frontline chemotherapy treatment. While they are a promising option for less toxic therapeutic
33 approaches, little is known about the effects of immune checkpoint inhibitors on reproductive and
34 endocrine function.

35 *Results:* Our findings in a syngeneic TNBC mouse model revealed that therapeutically relevant
36 immunotherapies targeting PD-1, LAG-3, and TIM-3 had no effect on the quality and abundance
37 of ovarian follicles, estrus cyclicity, or hormonal homeostasis. Similarly, in a tumor-free mouse
38 model, we found that ovarian architecture, follicle abundance, estrus cyclicity, and ovulatory
39 efficiency remain unchanged by PD-1 blockade.

40 *Conclusions:* Taken together, our results suggest that immunotherapy may be a promising
41 component of fertility-sparing therapeutic regimens for patients that wish to retain ovarian and
42 endocrine function after cancer treatment.

43

44 **KEYWORDS**

45 breast cancer, TNBC, PD-1 inhibitor, immune checkpoint inhibition, oncofertility, ovarian reserve

46

47

48

49

50

51

52

53 INTRODUCTION

54 Representing 15-20% of all breast cancer cases, triple negative breast cancer (TNBC) is
55 an aggressive form of breast cancer that is diagnosed more frequently in reproductive-age women
56 than other sub-types^{1,2}. Because TNBC lacks expression of the estrogen receptor (ER),
57 progesterone receptor (PR), and human epidermal growth factor receptor 2 (HER2), it is
58 unresponsive to many of the targeted treatments that are used for other subtypes of breast
59 cancer^{3,4}. Thus, cytotoxic chemotherapies, which are associated with several severe systemic
60 side effects, are often key components of frontline treatments⁵. Indeed, these side effects can
61 impact the reproductive system, and many as half of women who receive conventional
62 chemotherapies experience reproductive and endocrine dysfunction as a result⁶. However, recent
63 advances in cancer immunotherapy have led to the rapid integration of Pembrolizumab, a
64 programmed cell death protein 1 (PD-1) inhibitor, into standard-of-care treatment regimens for
65 TNBC, which may allow for reduced toxicity during treatment^{7,8}.

66 The development of immunotherapies has shown great promise for the targeted treatment
67 of a variety of cancers, and they lack many of the side effects observed with standard of care
68 chemotherapeutics⁹. One such class of immunotherapies that have seen clinical success is
69 immune checkpoint inhibitors, which target immune checkpoint regulators such as PD-1 and its
70 ligand PD-L1⁵. These ligands act as modulators in normal tissue to promote self-tolerance but are
71 overexpressed in tumor cells as a mode of evading immunosuppression¹⁰. Immune checkpoint
72 inhibitors such as Pembrolizumab employ monoclonal antibodies to block immune checkpoint
73 interactions with the goal of activating tumor-specific cytotoxic T cells and promoting immune cell-
74 mediated killing⁴.

75 Though the introduction of immune checkpoint inhibitors has revolutionized cancer
76 treatment paradigms and patient quality of life, the systemic blocking of immune checkpoint
77 interactions can cause immune-related adverse events (irAEs) associated with a lack of immune
78 tolerance of self-tissues¹¹. While these effects are not as common as those associated with

79 cytotoxic chemotherapy and are usually mild, they can occasionally be severe and may affect a
80 variety of organs systems⁹. Indeed, endocrine irAEs are some of the most commonly reported
81 irAEs in the clinic and include hyper- and hypothyroidism, hypophysitis, hypogonadism, and Type
82 I diabetes^{12,13}. In a 2022 study by Winship et al., anti-CTLA-4 and anti-PD-L1 monoclonal
83 antibodies were associated with an increase in intra-ovarian immune cells and tumor necrosis
84 factor- α (TNF- α) expression, as well as a decrease in ovarian follicle quality and abundance¹⁴.
85 However, no studies have evaluated the ovarian and endocrine effects of standard-of-care PD-1
86 inhibitors or blockade of other exploratory targets such as lymphocyte-activation gene 3 (LAG-3)
87 or T cell immunoglobulin and mucin domain 3 (TIM-3).

88 In the mammalian ovary, immature oocytes are stored in a quiescent state as primordial
89 follicles in a finite population known as the ovarian reserve^{15,16}. After puberty, these primordial
90 follicles are continuously activated to begin folliculogenesis, the process of transforming into
91 larger, mature follicles that produce steroid hormones and may eventually be ovulated^{17,18}. This
92 process occurs continuously through the entire reproductive lifespan until the ovarian reserve is
93 depleted, at which point menopause begins^{19,20}. Because new oocytes cannot be generated after
94 birth, it is critical that primordial follicles must be available in sufficient amounts and be maintained
95 through the reproductive lifespan of the host to ensure fertility and endocrine function^{21,22}.
96 Cytotoxic chemotherapies are among the foremost causes of ovarian reserve damage, often
97 resulting in the condition of Primary Ovarian Insufficiency (POI)^{6,23}. Caused by the depletion of
98 the ovarian reserve, POI can lead to infertility and impaired endocrine function, and increases the
99 risk of conditions associated with aging such as heart attack, stroke, and osteoporosis²⁴.

100 In all mammals, ovarian follicles undergo highly-conserved processes of growth,
101 maturation, ovulation, and death, although the timeline of these events is species-specific^{16,17}. In
102 humans, the time for an activated primordial follicle to mature into a fully-grown pre-ovulatory
103 follicle takes about 12 months, while in mice, this process takes around 21 days^{25,26}. The
104 menstrual cycle in humans takes an average of 28 days and typically results in the ovulation of a

105 single oocyte per cycle, while the mouse estrous cycle takes only 4-5 days and results in the
106 ovulation of several oocytes per cycle^{19,26}. The mouse reproductive cycle begins around 6-8
107 weeks of age and ends approximately after 12 months^{26,27}. In humans, the menstrual cycle begins
108 at the onset of puberty and continues until menopause^{16,19}. Though mice do not undergo a true
109 “menopause”, they experience similarities to human females in the processes of ovarian reserve
110 depletion, loss of fertility, and endocrine dysfunction with aging, and are therefore tremendously
111 useful models for study of mammalian reproductive function²⁸.

112 Immune regulation plays an important role in reproductive and endocrine health. The
113 ovary is subject to immune cell infiltration as it is a highly vascularized, non-immunoprivileged
114 organ²⁹. In the ovary, immune cells are critical in processes related to granulosa cell turnover,
115 ovulation, clearing atretic follicles, and the development and breakdown of the corpus luteum^{30,31}.
116 In addition, signaling by cytokines such as TNF- α and transforming growth factor- β (TGF- β) are
117 crucial in follicle maturation and ovulation²⁰. However, it is likely that dysregulation or over-
118 activation of these immune factors could cause damage to the ovary³²⁻³⁴. A few epidemiologic
119 studies have reported a higher incidence of POI and unexplained infertility in women with chronic
120 inflammatory or autoimmune conditions such as Crohn’s Disease and psoriasis^{35,36}. In addition,
121 there is some evidence linking inflammation and autoimmunity on ovarian aging and follicle
122 depletion in animal models³⁴. However, the specific mechanisms of autoimmune depletion of the
123 ovarian reserve remain unknown, and it is unclear whether immune checkpoint inhibitor treatment
124 creates a sufficiently heightened systemic immune response to elicit ovarian damage and
125 endocrine disruption.

126 The ovarian toxicity of many of the frontline chemotherapeutics for TNBC has been well-
127 characterized, with the non-renewable population of oocytes being some of the most vulnerable
128 cells to damage^{6,23}. As immune checkpoint inhibitors continue to be incorporated into clinical
129 practice, more studies on their reproductive and endocrine effects are necessary, especially if
130 they are to be used as a component of fertility-sparing treatment regimen. Moreover, given the

131 fact that they are still relatively new to the cancer therapeutic repertoire, data on long-term fertility
132 outcomes in human TNBC patients treated with immune checkpoint inhibitors is not yet available
133 and thus preclinical models must be used to evaluate their ovarian impacts³⁷. We hypothesized
134 that ICIs targeting PD-1, LAG-3 and TIM-3 would be relatively benign to ovarian reserve and
135 endocrine function.

136

137 **MATERIAL AND METHODS**

138 *Animals*

139 Wild-type C57Bl/6 mice were obtained from the Jackson Laboratory (strain # 000664). All
140 animal protocols were approved by Brown University Institutional Animal Care and Use
141 Committee and were performed in accordance with the National Institutes of Health Guide for the
142 Care and Use of Laboratory Animals (# 22-09-0002). All animal protocols were reviewed and
143 acknowledged by the Lifespan University Institutional Care and Use Committee (# 1987412-1).

144

145 *E0771 tumor-bearing mouse model and tissue collection*

146 Mouse E0771 cells were obtained from ATCC and cultured in DMEM, 10% FBS, and
147 penicillin/streptomycin. Cells were found to be free of pathogens and mycoplasma (per Charles
148 River pathogen testing). Eight-week-old female C57Bl/6J mice were injected with 100 μ L of 1×10^5
149 E0771 cell suspension in Matrigel or saline control into the bilateral 4th mammary pads under
150 isoflurane sedation. Once palpable 14 days later, a group of pre-treatment mice were collected,
151 and remaining mice were randomly allocated into study groups to begin treatment regimen of
152 immune checkpoint inhibitor monotherapy or control. Mice received 200 μ g doses of mouse anti-
153 PD-1 (clone: 29F.1A12), anti-LAG-3 (clone: C9B7W), anti-TIM-3 (clone: RMT3-23), or rat IgG2a
154 isotype control (clone: 2A3) every 4 days via intraperitoneal injection, with treatments stopping
155 after the third dose. All antibodies used for *in-vivo* treatments were purchased from BioXcell.
156 Doses were based on previously described tumor-reducing regimens⁴⁵. Mice were monitored for

157 14 days and then collected once they reached proestrus stage. Upon collection, tumors, ovaries,
158 and serum were obtained for further analysis. Tumor burden was determined by quantifying tumor
159 weight as a proportion of total mouse weight.

160

161 *Non-tumor-bearing mouse model and tissue collection*

162 Eight-week-old female C57Bl/6J mice were mock-injected with 100 μ L saline in the 4th
163 mammary pad under isoflurane sedation. 14 days later, mice were randomly allocated into study
164 groups to begin treatment with anti-PD-1 monoclonal antibody, IgG isotype control, or saline via
165 intraperitoneal injection. Mice in the anti-PD-1 and IgG isotype control group received 200 μ g
166 doses of monoclonal antibodies every 4 days via intraperitoneal injection, with treatments
167 stopping after the third dose. Mice were monitored for 14 days and then collected once they
168 reached proestrus stage. Upon collection, ovaries and serum were obtained for further analysis.

169

170 *Vaginal cytology and estrus cycle analysis*

171 After the final dose of immunotherapy or control, estrus cycle stage was monitored daily
172 over the course of 14 days via vaginal smear cytology as previously described⁴⁶. Briefly, the
173 vagina of each mouse was flushed with saline and then mixed with toluidine blue O dye on a glass
174 slide, then classified into the different sub-stages of estrus based on the cell types visualized in
175 the sample. The percentage of time spent in each sub-stage of estrus was calculated for each
176 mouse and results were compared between treatment groups.

177

178 *Ovarian histology and follicle quantification*

179 Ovaries from tumor-bearing and non-tumor-bearing mice were stained and analyzed as
180 previously described⁴⁶. Briefly, ovaries were fixed in formalin and embedded in paraffin for
181 sectioning at 5 μ m by the Brown Molecular Pathology Core, and every fourth slide was
182 deparaffinized and stained with hematoxylin and eosin (H&E). Five slides per ovary were

183 quantified. Follicles were staged and counted on one section per every H&E-stained slide, and
184 these counts were normalized to section area to yield follicle density.

185

186 *TUNEL staining*

187 Prior to staining, ovarian FFPE slides were deparaffinized as previously described. Slides
188 were then washed for 3 minutes in Phosphate Buffered Saline (PBS), then permeabilized by
189 applying freshly prepared 20 µg/mL Proteinase K in 10mM Tris-HCl solution and incubating for
190 15 minutes in a humid chamber at room temperature. Slides were then washed 2x, 3 minutes in
191 PBS, 1x 3 minutes in PBS + 0.1% Triton (PBST), then again 2x, 3 minutes in PBS. Slides were
192 then stained with the *In Situ Cell Death Detection Kit, Fluorescein* (Roche) according to
193 manufacturer's instructions. Briefly, slides were incubated with TUNEL reaction mixture for 1 hour
194 in a humid chamber at 37°C protected from light. Slides were then washed 3x for 3 minutes in
195 PBS, once for 3 minutes in DAPI/PBS solution, and then once for 5 minutes in PBS. Slides were
196 then mounted and analyzed on an EVOS M5000 Fluorescence Imaging System and images of
197 all fields of a single section were captured.

198

199 *Serum hormone analysis*

200 Whole blood from mice was collected via post-mortem cardiac puncture and serum
201 separated out as previously described⁴⁶. Serum was sent to the University of Virginia Ligand
202 Assay & Analysis Core for the Center for Research in Reproduction for quantification of serum
203 concentrations of AMH, LH, and FSH.

204

205 *Superovulation of tumor-bearing and non-tumor-bearing mice*

206 For superovulation experiments in tumor-bearing mice, eight-week-old wild-type C57Bl/6J
207 mice were orthotopically injected with E0771 cells into the right 4th mammary pad as previously
208 described. Once palpable 14 days later, mice were randomly allocated into groups to receive

209 intraperitoneal injections of anti-200 µg doses of PD-1 monoclonal antibody or IgG isotype control,
210 or 100 µL of saline control every 4 days with treatments stopping after the third dose. Eight days
211 after receiving their final dose, mice underwent ovarian hyperstimulation as previously
212 described⁴⁶. Briefly, mice were injected with 5-IU pregnant mare goat serum (PMSG; Prospec
213 Bio), and then 48 hours later, injected with 5-IU human chorionic gonadotropin (HCG; Prospec
214 Bio). Twelve hours after HCG injection, mice were euthanized, and ovulated oocytes were
215 collected from the ampullae. Number of oocytes ovulated were counted per mouse and results
216 were compared between treatment groups.

217

218 For superovulation experiments in non-tumor-bearing mice, six-week-old wild-type
219 C57Bl/6J mice were mock-injected with saline into the mammary pad as described. As with the
220 tumor-bearing superovulation study, mice were randomly allocated into groups 14 days later to
221 receive intraperitoneal injections of anti-200 µg doses of PD-1 monoclonal antibody or IgG isotype
222 control, or 100 µL of saline control every 4 days with treatments stopping after the third dose.
223 Eight days after receiving their final dose, mice underwent ovarian hyperstimulation and ovulated
224 oocytes were quantified as described.

225

226 *Statistical analysis*

227 Ovarian area and follicle density were quantified from H&E-stained ovarian sections.
228 Follicles were counted by stage, and these counts were then normalized to the section area to
229 calculate oocyte density and account for size differences between different ovaries. For estrus
230 cycling analyses, the percentage of time spent in each substage was then averaged between all
231 animals in a treatment group. For superovulation studies, recovered oocytes were quantified and
232 averaged per treatment group, and mice were classified as “successfully stimulated” if the number
233 of retrieved oocytes met an age-adjusted threshold based on average litter sizes for wild-type
234 C57Bl/6J mice in our lab (7 oocytes for 8-week-old mice, 10 oocytes for 6-week-old mice). One-

235 way ANOVA with post-hoc Tukey's tests for multiple comparisons were performed to evaluate
236 differences in tumor burden, follicle abundance, serum hormone levels, percentage of time spent
237 in estrus between treatment groups.

238

239 **RESULTS**

240 *Inhibition of PD-1, LAG-3, and TIM-3 does not impact ovarian follicle abundance or quality in a*
241 *mouse model of triple negative breast cancer*

242 To assess the effects of immune checkpoint inhibition on ovarian health and endocrine
243 function in a clinically-relevant model of TNBC, we collected ovaries and serum of C57Bl/6J mice
244 who had been orthotopically injected with syngeneic E0771 cells into the mammary pad, then
245 treated with intraperitoneal injections of anti-PD-1, anti-LAG-3, or anti-TIM-3 monotherapy. These
246 immunotherapies represent an array of immune checkpoint inhibitor candidates that have
247 demonstrated varying efficacy in clinical trials for solid cancers, with anti-PD-1 being the most
248 effective in TNBC populations³⁸⁻⁴⁰. By choosing these specific targets, we were able to
249 comprehensively evaluate the effects of differential immune activation on the ovarian reserve and
250 hormonal homeostasis. Tumor-bearing control group mice received intraperitoneal injections of
251 IgG isotype at the same timepoints as immunotherapy-treated mice, and healthy control mice only
252 received a mock-injection of saline into the mammary pad at the time of orthotopic injections. To
253 control for cycle stage-dependent fluctuations in folliculogenesis, ovaries were collected during
254 the proestrus stage 14-16 days following the final immunotherapy treatment. This collection
255 timepoint allowed us to capture any effects that may have a pattern of delayed onset seen in
256 some other adverse immune effects.

257 Morphologically, ovarian architecture was similar among all treatment groups (Fig 1a-f).
258 Follicles were classified by stage, including the immature, quiescent primordial follicles that make
259 up the ovarian reserve, the developing primary, secondary, and preantral follicles that have been
260 recruited and activated to undergo maturation, and the antral follicles that are nearly ready for

261 ovulation. Degenerative follicles, which are undergoing atresia and dying, were also quantified
262 per section. At the post-treatment timepoint, anti-PD-1-treated mice showed almost complete
263 tumor regression, which was statistically significant when compared to the IgG isotype control
264 group ($p=0.0125$) (Fig 1f). Mice treated with anti-LAG-3 or anti-TIM-3 exhibited a more variable
265 response to treatment, with the anti-TIM-3-treated group achieving a significant reduction in tumor
266 burden ($p=0.0492$). Though the anti-LAG-3 group had a lower mean tumor burden than IgG
267 isotype controls, this difference was not statistically significant ($p=0.8006$). Ovarian area, as well
268 as overall and stage-specific oocyte densities were not significantly different between immune
269 checkpoint inhibitor-treated groups and IgG isotype-treated or saline mock-injected controls (Fig
270 1g-i). There were also no appreciable levels of oocyte or granulosa cell apoptosis found via
271 TUNEL staining (Supp Fig 1). These findings indicate that inhibition of a variety of immune
272 checkpoint interactions has no long-term effect on ovarian morphology or folliculogenesis in a
273 tumor-bearing system.

274

275 *Inhibition of PD-1, LAG-3, or TIM-3 does not perturb endocrine homeostasis or reproductive*
276 *cyclicality*

277 Given that long-term endocrine dysfunction and disruption of reproductive cycling are
278 common side effects of cancer therapy that are at times unrelated to ovarian reserve function, we
279 assessed these outcomes via serum hormone and estrus cycling analysis in the E0771 tumor-
280 bearing mouse model. As with the ovarian collections, we collected serum during the proestrus
281 stage 14-16 days following the final immunotherapy treatment to control for cycle stage-
282 dependent fluctuations in hormone levels. Serum levels of luteinizing hormone (LH) and follicle
283 stimulating hormone (FSH) were quantified to evaluate possible disturbances in the hypothalamic-
284 pituitary-gonadal axis and hormonal cycling. Serum levels of anti-Mullerian hormone (AMH),
285 produced by granulosa cells of maturing follicles and current clinical gold standard for evaluating
286 follicle abundance, was also quantified⁴¹. Serum levels of LH and FSH levels did not differ

287 significantly between any of the immunotherapy treatment and control groups (Fig 2a-b).
288 Likewise, there were no significant differences observed in LH:FSH ratio (Fig 2c), a common
289 clinical metric in which high values correlate with a lack of ovulation in polycystic ovarian
290 syndrome⁴². Consistent with our ovarian follicle density results, we found that AMH levels were
291 unchanged between immunotherapy-treated and control group animals.

292 Estrus cyclicity was analyzed by monitoring vaginal cytology daily for two weeks starting
293 the day after the final immunotherapy or IgG isotype control treatment. We found that there were
294 no significant differences in the amount of time spent in each of the cycle stages between any of
295 the immunotherapy treatment and control groups (Figure 2e). Taken together with the serum
296 hormone data, these findings suggest that immune checkpoint blockade does not impair
297 endocrine function or hormonal cyclicity in tumor-bearing mice.

298

299 *Treatment with anti-PD-1 immunotherapy does not impact ovarian follicle density or reproductive*
300 *cyclicity in a non-tumor-bearing mouse model*

301 To further investigate ovarian and endocrine function after treatment with anti-PD-1
302 immunotherapy and to disentangle any observed effects from tumor burden-specific phenomena,
303 we sought to validate our results in a tumor-free mouse model. To simulate orthotopic implantation
304 of tumor cells, young adult female C57Bl/6J mice age-matched to the E0771 cohort were mock-
305 injected with saline into the mammary pad. Narrowing down our treatment focus to answer
306 questions of key clinical relevancy, we then administered anti-PD-1 mAb, IgG isotype control, or
307 saline control intraperitoneal injections, all at the same timepoints as the cohort of E0771 tumor-
308 bearing mice. As with all tumor-bearing studies, ovaries and serum collected 14-16 days following
309 the final treatment when mice entered the proestrus stage.

310 Ovaries from all groups of non-tumor-bearing mice appeared morphologically similar to
311 each other (Fig 3a-c) and showed no differences in total area (Fig 3d). Upon quantifying ovarian
312 follicle abundance, anti-PD-1-treated mice did not differ significantly in oocyte and follicle stage

313 densities compared to IgG isotype and saline-treated controls (Fig 3e-f). These findings
314 recapitulate our results from the tumor-bearing model and suggest that PD-1 blockade has no
315 negative effect on follicle abundance or folliculogenesis.

316 To evaluate any effects of anti-PD-1 immunotherapy on hormonal cyclicity in the absence
317 of tumor burden, we monitored estrus cycling via vaginal cytology for two weeks following
318 administration of the final immunotherapy or control treatment. Unsurprisingly, we found that the
319 percentage of time spent in each substage of estrus was unchanged between anti-PD-1-treated
320 animals and control animals treated with IgG isotype or saline (Fig 3g). These results are
321 consistent with the tumor-bearing model, suggesting that hormonal cyclicity is unaffected by PD-
322 1 inhibition in both a tumor-bearing and non-tumor-bearing system.

323 Interestingly, the only differences observed in ovarian composition are found when
324 comparing treatment-matched groups from the tumor-bearing and non-tumor-bearing cohorts.
325 IgG isotype-treated animals from the tumor-bearing group have a statistically significant decrease
326 in ovarian area compared to their non-tumor-bearing counterparts (Supp Fig 2). Likewise, tumor-
327 bearing anti-PD-1-treated animals had higher levels of preantral follicle density than the non-
328 tumor-bearing anti-PD-1-treated group (Supp Fig 2). These findings demonstrate that the effect
329 of tumor burden may play a larger role in determining ovarian and endocrine health than any
330 immune-related changes resulting from PD-1 blockade.

331

332 *Treatment with anti-PD-1 immunotherapy does not impair ovulatory capacity*

333 To investigate whether PD-1 inhibition could affect ovulatory efficiency, we conducted
334 superovulation studies to assess responses to ovarian hyperstimulation. One week following
335 treatment with anti-PD-1 immunotherapy, IgG isotype, or saline control, animals of each group
336 were hormonally stimulated with PMSG, then given a trigger shot of HCG 48 hours later. Cumulus-
337 oocyte complexes and ovaries were collected from the ampullas of all animals 12 hours after the

338 HCG injection. Ovaries from stimulated mice displayed corpora lutea formation consistent with
339 recent ovulation (Fig 4 a-c).

340 There were no significant differences in the numbers of successfully stimulated mice or
341 number of oocytes recovered per stimulated mouse between the anti-PD-1-treated group and
342 control groups (Fig 4d-e). These results indicate that PD-1 inhibition does not impact ovulatory
343 efficiency or the ability to respond to hormonal stimulation.

344

345 **DISCUSSION**

346 As cancer therapeutics and survivorship outcomes improve, preserving the ovarian
347 reserve during cancer treatment has become critical. Not only does the ovarian reserve comprise
348 an individual's entire reproductive potential, but it also directly contributes to endocrine balance,
349 making it critical for female health-span and lifespan. Moreover, though immune checkpoint
350 inhibitors may potentially be a less-toxic approach to treating cancer, they are still associated with
351 a suite of adverse immune effects and thus require characterization of their impact on
352 reproductive and hormonal function^{2,13}. Based on our rigorous studies in both a TNBC tumor-
353 bearing model and a tumor-free model, we found no evidence that immune checkpoint inhibition
354 negatively affects the ovarian reserve or endocrine homeostasis.

355 In this work, we demonstrate that ovarian architecture and follicle density remain
356 unchanged by immune checkpoint blockade. Ovaries from tumor-bearing mice treated with
357 immunotherapies targeting PD-1, LAG-3, and TIM-3 appeared healthy and bore remarkable
358 resemblance to ovaries from mice treated with IgG isotype control. While we were interested in
359 understanding any ovarian or endocrine effects of anti-PD-1 therapy as it is commonly being used
360 to treat TNBC in the clinic, we chose to also investigate anti-LAG-3 and anti-TIM-3 because of
361 their possible future uses in treatment regimens for TNBC or other solid cancers. However, due
362 to their variable efficacy in TNBC clinical trials, we narrowed our scope to focus solely on anti-
363 PD-1 therapy in non-tumor-bearing and subsequent studies³⁸. As seen in the tumor-bearing

364 cohort, ovaries from non-tumor-bearing mice treated with anti-PD-1 were equally as healthy as
365 the control group ovaries. Critically, this lack of ovarian and endocrine damage observed after
366 immune checkpoint inhibitor treatment coincides with tumor regression in the tumor-bearing
367 cohort, particularly in anti-PD-1-treated mice. This anti-tumor efficacy indicates that our
368 monotherapy doses are therapeutically relevant, and thus, are appropriate doses for evaluating
369 reproductive toxicity.

370 Interestingly, the primary differences were found only when comparing ovaries from tumor-
371 bearing mice to those from non-tumor-bearing mice. Among mice treated with anti-PD-1 therapy,
372 preantral follicles were significantly higher in the tumor-bearing group, while non-significant
373 increases could also be seen in degenerative and primary follicles of the tumor-bearing group.
374 One possible reason for this could be a delay in follicle maturation in tumor-bearing animals,
375 causing an accumulation of maturing follicles and thus a higher percentage of degeneration.
376 These disruptions in folliculogenesis may be attributable to non-specific inflammation related to
377 tumor burden, especially considering the anatomical proximity of the mammary tumor to the
378 ovaries. Moreover, among mice treated with IgG isotype, ovarian area was reduced in the tumor-
379 bearing group while oocyte density remained comparable. This finding could potentially be due to
380 cancer-related inflammatory effects on the somatic compartment of the ovary, a mechanism
381 proposed by Chaqour et al⁴³. These results may possibly indicate a trend that local cancer-
382 associated inflammation may have a larger role in determining ovarian health than immune
383 checkpoint blockade itself.

384 Our studies also show that hormonal cyclicity and serum hormone levels are similar
385 between immunotherapy and control group mice. These results were not particularly surprising
386 given that we found that immunotherapy did not diminish the ovarian reserve. However,
387 considering that autoimmune disorders affecting endocrine function are among the most common
388 of the adverse immune effects associated with immune checkpoint inhibitor treatment, it was
389 important for our research to investigate possible extra-ovarian effects¹³. Finally, our results

390 suggest that anti-PD-1 immunotherapy has no effect on responsiveness to hormonal stimulation
391 or ovulatory capacity. Taken together, we can conclude that immune checkpoint inhibitors, namely
392 anti-PD-1-based immunotherapies, could be a critical component of ovary-sparing cancer
393 therapeutic regimens.

394 Though there is little literature available on the effects of immunotherapy on the ovarian
395 reserve, a 2022 study from Winship et al. found that PD-L1 and CTLA-4 inhibition causes
396 depletion of the ovarian reserve, disruption of estrus cyclicity, reduced ovulatory capacity, and an
397 increase in intra-ovarian immune activity¹⁴. Similar to our studies, Winship et al. evaluated these
398 immunotherapies in both a tumor-bearing and non-tumor-bearing model. Given that we
399 investigated different immune checkpoint targets, our results are not necessarily inconsistent with
400 those reported by Winship et al. However, our conclusions are strikingly different when
401 generalizing about the effects of immune checkpoint blockade as a whole. While the Winship
402 study posits that immune checkpoint inhibitors are harmful to the ovarian reserve, our study is the
403 first to test the effects of anti-PD-1 therapy, the only standard-of-care immunotherapy approved
404 by the FDA for the treatment of TNBC⁷. In addition to the difference in selection of immune
405 checkpoint targets, some of our contrasting results may also be attributable to the difference in
406 mouse models used. For example, the Winship study employed the use of C57Bl/6J mice
407 orthotopically injected with AT3OVA cells for their tumor-bearing experiments¹⁴. While this is
408 indeed a syngeneic model for mammary carcinoma, the cell line is not as commonly used as our
409 E0771 model and could have critical differences in immunogenicity, receptor expression, or
410 clinical relevance⁴⁴. Ultimately, our study provides critical context to the current body of
411 knowledge on the reproductive and endocrine impact of immune checkpoint inhibitors.

412 Our mouse studies sought to model a clinically-relevant dosing schedule equivalent to one
413 round of immunotherapy treatment widely used in previous research. By allowing 14 days to
414 elapse between treatment and collection, we were able to monitor and record daily estrus cycling
415 to assess immediate effects before eventually capturing delayed effects on ovarian health and

416 serum hormone balance. Future studies will target long-term outcomes such as fecundity and
417 premature ovarian aging after immunotherapy exposure.

418 Though we aimed to design and execute comprehensive studies, this work is not without
419 its limitations. Our studies do not investigate subtle immunotherapy-induced changes that may
420 not be apparent in histological analyses. However, due to the overwhelming lack of negative
421 functional effects observed, any subtle phenotypes will be subject of future studies and are
422 beyond the purview of this current study. In addition, we recognize that the number of mice who
423 were responsive to hormonal stimulation is low, making it more difficult to draw conclusions about
424 ovulatory capacity. However, considering the need to balance a clinically-relevant dosing schema
425 with the inherent challenges of hormonally stimulating mice older than 4 weeks of age, we chose
426 to perform our study as described and make statistical adjustments to account for reasonable
427 oocyte recoveries.

428

429 **CONCLUSIONS**

430 Our research adds novel information to a burgeoning field studying the effects of
431 immunotherapy on reproductive and endocrine function, and provides reassuring data to support
432 that anti-PD-1 therapy for TNBC, which is now standard-of-care, does not detrimentally affect
433 ovarian function. Given the rising number of young women being diagnosed with TNBC, there is
434 a critical need to design treatment approaches that can maximize therapeutic efficacy while
435 minimizing damage to the ovarian reserve, thereby improving treatment outcomes and quality of
436 life for survivors. Though population-level clinical data would provide the most clarity on the fertility
437 outcomes after immune checkpoint inhibitor treatment, our studies present a human-relevant
438 animal model to assess ovarian and endocrine effects of novel immunotherapies to inform clinical
439 recommendations.

440

441 **DECLARATIONS**

442 *Ethics approval and consent to participate*

443 Not applicable.

444

445 *Consent for publication*

446 Not applicable.

447

448 *Availability of data and materials*

449 The data generated from this study are available from the corresponding author upon reasonable
450 request.

451

452 *Competing interests*

453 The authors declare no competing interests.

454

455 *Funding*

456 Primary sources of funding for personnel, reagents, and supplies was provided by Swim Across
457 America and the Foundation for Women's Wellness. Support for key instruments used for this
458 research was provided by the Kilguss Research Core of Women and Infants Hospital and the
459 Brown University Genomics Core.

460

461 *Authors' contributions*

462 PDLC, MFW-S, JNM, ES, LH, MMA, and KJG performed the experiments. PDLC and KJG
463 analyzed and interpreted the data. PDLC and KJG wrote and revised the manuscript.

464

465 *Acknowledgements*

466 The authors would like to thank the Program in Women's Oncology of Women and Infants Hospital
467 and the generous funding support of Swim Across America and the Foundation for Women's

468 Wellness. Technical support for this work was provided by the University of Virginia Center for
469 Research in Reproduction Ligand Assay and Analysis Core, which is supported by the Eunice
470 Kennedy Shriver NICHD Grant R24 HD102061. The authors thank the Freiman and James
471 laboratories for providing valuable feedback on this project.
472

473 **FIGURE LEGENDS**

474 *Figure 1- Inhibition of PD-1, LAG-3, and TIM-3 does not impact ovarian follicle abundance or*
475 *quality in a mouse model of triple negative breast cancer*

476 Ovaries from E0771 tumor-bearing mice treated with monoclonal antibodies targeting PD-1, LAG-
477 3, TIM-3 (**A-C**), IgG isotype (**D**), and a healthy control mock-injected with saline (**E**) were collected,
478 formalin-fixed, paraffin-embedded, and then stained with hematoxylin and eosin via standard
479 protocols (n=3 per group). Degenerative follicles are denoted with white arrows. Tumor burden
480 analysis (**F**) at study endpoint reveals near-complete tumor regression in anti-PD-1-treated mice,
481 along with varying reductions in tumor size in the anti-LAG-3 and anti-TIM-3 groups (n=3 per
482 treatment group). Ovarian size, oocyte density, and follicle stage density was not significantly
483 different between any of the treatment or control groups (**G-I**). Ovarian follicle counts were
484 quantified using one section on every fourth slide of sectioned ovary to capture all follicle stages
485 without over-representing larger follicles. To account for size differences between ovaries, section
486 area was used to normalize follicle counts. Data for follicle counts, follicle density, and ovarian
487 area can be found in Supplementary File 1.

488 *p<0.05, as indicated,

489

490 *Figure 2- Inhibition of PD-1, LAG-3, and TIM-3 does not perturb endocrine homeostasis or*
491 *reproductive cyclicity*

492 Serum concentrations of LH (**A**) and FSH (**B**), as well as the LH:FSH ratio (**C**), and AMH (**D**) were
493 not significantly different between any of the treatment and control groups (n=3 per group). Estrus
494 cyclicity was monitored daily via vaginal cytology for two weeks starting the day following the final
495 immunotherapy treatment, and the percentage of time spent in each substage was averaged
496 between mice in each treatment group (n=3 per group). The amount of time spent in each
497 substage of the estrus cycle was unchanged between all treatment and control groups (**E**).

498

499 *Figure 3- Treatment with anti-PD-1 immunotherapy does not impact ovarian follicle density or*
500 *reproductive cyclicity in a non-tumor-bearing mouse model*

501 Ovaries were collected for FFPE from healthy, non-tumor-bearing mice treated with anti-PD-1
502 monoclonal antibodies, IgG isotype control, or saline control (**A-C**), and then stained with
503 hematoxylin and eosin (n= 3 per group). There were no significant differences between ovarian
504 size, oocyte density, follicle abundance, or the percentage of time spent in each substage of
505 estrus between treatment groups (**D-G**). Data for follicle counts, follicle density, and ovarian area
506 can be found in Supplementary File 2.

507

508 *Figure 4- Treatment with anti-PD-1 immunotherapy does not impair ovulatory capacity*

509 One week following treatment with anti-PD-1 monoclonal antibodies, IgG isotype control, or saline
510 control, mice were super-ovulated with PMSG and HCG using standard protocols. Ovaries from
511 superovulated mice were collected for FFPE and then stained with hematoxylin and eosin (**A-C**).
512 There were no significant differences in the number of mice who responded to hormonal
513 stimulation (**D**) or the number of oocytes retrieved from successfully superovulated mice (**E**).
514 Retrieved oocytes were collected from each animal, then counted and averaged per treatment
515 group (n=6 for anti-PD-1 and IgG isotype control, n=5 for saline control). Mice were classified as
516 “successfully stimulated” if their number of retrieved oocytes reached an age-adjusted threshold
517 for hyperstimulation (10 oocytes for 7-week-old mice, 7 oocytes for 10-week-old mice). Counts of
518 retrieved oocytes from “successfully stimulated” mice were averaged and compared between
519 treatment groups (n=5 for anti-PD-1, n=2 for IgG isotype control, n=4 for saline control).

520

521 *Supplemental figure 1*

522 TUNEL staining of ovaries from E0771 tumor-bearing mice treated with monoclonal antibodies
523 targeting PD-1, LAG-3, TIM-3, and IgG isotype control showed no appreciable levels of apoptosis
524 in follicles.

525

526 *Supplemental figure 2*

527 Differences in ovarian area, follicle density, and estrus cyclicity in tumor-bearing vs. non-tumor-
528 bearing mice. Among mice treated with IgG isotype control, ovarian area was significantly
529 increased in non-tumor-bearing mice, which may indicate increased volume in the ovarian
530 somatic compartment of healthy mice. Among mice receiving anti-PD-1 treatment, preantral
531 follicle counts were significantly higher in the tumor-bearing group, perhaps indicating an
532 accumulation of maturing follicles in TNBC mice.

533 * $p < 0.05$, as indicated

534

535 **REFERENCES**

- 536 1. American Cancer Society. About Breast Cancer. *Am Cancer Soc Cancer Facts Fig Atlanta,*
537 *Ga Am Cancer Soc.* Published online 2017:1-19. [http://www.cancer.org/cancer/breast-](http://www.cancer.org/cancer/breast-cancer/about/what-is-breast-cancer.html)
538 [cancer/about/what-is-breast-cancer.html](http://www.cancer.org/cancer/breast-cancer/about/what-is-breast-cancer.html)
- 539 2. Duma N, Lambertini M. It Is Time to Talk About Fertility and Immunotherapy. *Oncologist.*
540 2020;25(4):277-278. doi:10.1634/theoncologist.2019-0837
- 541 3. Yin L, Duan JJ, Bian XW, Yu SC. Triple-negative breast cancer molecular subtyping and
542 treatment progress. *Breast Cancer Res.* 2020;22(1):1-13. doi:10.1186/s13058-020-01296-
543 5
- 544 4. Kalimutho M, Parsons K, Mittal D, López JA, Srihari S, Khanna KK. Targeted Therapies for
545 Triple-Negative Breast Cancer: Combating a Stubborn Disease. *Trends Pharmacol Sci.*
546 2015;36(12):822-846. doi:10.1016/j.tips.2015.08.009
- 547 5. Singh S, Numan A, Maddiboyina B, et al. The emerging role of immune checkpoint
548 inhibitors in the treatment of triple-negative breast cancer. *Drug Discov Today.*
549 2021;26(7):1721-1727. doi:10.1016/j.drudis.2021.03.011
- 550 6. Morgan S, Anderson RA, Gourley C, Wallace WH, Spears N. How do chemotherapeutic
551 agents damage the ovary? *Hum Reprod Update.* 2012;18(5):525-535.
552 doi:10.1093/humupd/dms022
- 553 7. U.S. Food and Drug Administration. FDA approves pembrolizumab for high-risk early-stage
554 triple-negative breast cancer. Published 2021. [https://www.fda.gov/drugs/resources-](https://www.fda.gov/drugs/resources-information-approved-drugs/fda-approves-pembrolizumab-high-risk-early-stage-triple-negative-breast-cancer)
555 [information-approved-drugs/fda-approves-pembrolizumab-high-risk-early-stage-triple-](https://www.fda.gov/drugs/resources-information-approved-drugs/fda-approves-pembrolizumab-high-risk-early-stage-triple-negative-breast-cancer)
556 [negative-breast-cancer](https://www.fda.gov/drugs/resources-information-approved-drugs/fda-approves-pembrolizumab-high-risk-early-stage-triple-negative-breast-cancer)
- 557 8. Volckmar X, Vallejo M, Bertoldo MJ, et al. Oncofertility Information Available for Recently
558 Approved Novel Non Cytotoxic and Immunotherapy Oncology Drugs. *Clin Pharmacol Ther.*
559 2021;0(0):1-9. doi:10.1002/cpt.2254
- 560 9. Schirmacher V. From chemotherapy to biological therapy: A review of novel concepts to
561 reduce the side effects of systemic cancer treatment (Review). *Int J Oncol.* 2019;54(2):407-
562 419. doi:10.3892/ijo.2018.4661

- 563 10. Darvin P, Toor SM, Sasidharan Nair V, Elkord E. Immune checkpoint inhibitors: recent
564 progress and potential biomarkers. *Exp Mol Med*. 2018;50(12):1-11. doi:10.1038/s12276-
565 018-0191-1
- 566 11. Brown TJ, Mamtani R, Bange EM. Immunotherapy Adverse Effects. *JAMA Oncol*.
567 2021;7(12):1908. doi:10.1001/jamaoncol.2021.5009
- 568 12. Wright JJ, Powers AC, Johnson DB. Endocrine toxicities of immune checkpoint inhibitors.
569 *Nat Rev Endocrinol*. 2021;17(7):389-399. doi:10.1038/s41574-021-00484-3
- 570 13. Husebye ES, Castinetti F, Criseno S, et al. Endocrine-related adverse conditions in patients
571 receiving immune checkpoint inhibition: an ESE clinical practice guideline. *Eur J*
572 *Endocrinol*. 2022;187(6):G1-G21. doi:10.1530/EJE-22-0689
- 573 14. Winship AL, Alesi LR, Sant S, et al. Checkpoint inhibitor immunotherapy diminishes oocyte
574 number and quality in mice. *Nat Cancer*. 2022;3(8):1-13. doi:10.1038/s43018-022-00413-
575 x
- 576 15. Kerr JB, Myers M, Anderson RA. The dynamics of the primordial follicle reserve.
577 *Reproduction*. 2013;146(6). doi:10.1530/REP-13-0181
- 578 16. Grive KJ, Freiman RN. The developmental origins of the mammalian ovarian reserve. *Dev*.
579 2015;142(15):2554-2563. doi:10.1242/dev.125211
- 580 17. Pepling ME. Follicular assembly: Mechanisms of action. *Reproduction*. 2012;143(2):139-
581 149. doi:10.1530/REP-11-0299
- 582 18. Monniaux D, Clément F, Dalbiès-Tran R, et al. The ovarian reserve of primordial follicles
583 and the dynamic reserve of antral growing follicles: what is the link? *Biol Reprod*.
584 2014;90(4):85. doi:10.1095/biolreprod.113.117077
- 585 19. Richards JS, Pangas SA, Richards JS, Pangas SA. The ovary : basic biology and clinical
586 implications Find the latest version : Review series The ovary : basic biology and clinical
587 implications. 2010;120(4):963-972. doi:10.1172/JCI41350.critical
- 588 20. Edson MA, Nagaraja AK, Matzuk MM. The mammalian ovary from genesis to revelation.
589 *Endocr Rev*. 2009;30(6):624-712. doi:10.1210/er.2009-0012

- 590 21. Kerr JB, Brogan L, Myers M, et al. The primordial follicle reserve is not renewed after
591 chemical or γ -irradiation mediated depletion. *Reproduction*. 2012;143(4):469-476.
592 doi:10.1530/REP-11-0430
- 593 22. Grive KJ. Pathways coordinating oocyte attrition and abundance during mammalian
594 ovarian reserve establishment. *Mol Reprod Dev*. 2020;87(8):843-856.
595 doi:10.1002/mrd.23401
- 596 23. Bedoschi G, Navarro PA, Oktay K. Chemotherapy-induced damage to ovary: Mechanisms
597 and clinical impact. *Futur Oncol*. Published online 2016. doi:10.2217/fon-2016-0176
- 598 24. Wesevich V, Kellen AN, Pal L. Recent advances in understanding primary ovarian
599 insufficiency. *F1000Research*. Published online 2020.
600 doi:10.12688/f1000research.26423.1
- 601 25. Gougeon A. Dynamics of follicular growth in the human: a model from preliminary results.
602 *Hum Reprod*. 1986;1(2):81-87. doi:10.1093/oxfordjournals.humrep.a136365
- 603 26. Chaffin CL, VandeVoort CA. Follicle growth, ovulation, and luteal formation in primates and
604 rodents: A comparative perspective. *Exp Biol Med*. 2013;238(5):539-548.
605 doi:10.1177/1535370213489437
- 606 27. Byers SL, Wiles M V., Dunn SL, Taft RA. Mouse estrous cycle identification tool and
607 images. *PLoS One*. 2012;7(4):2-6. doi:10.1371/journal.pone.0035538
- 608 28. Coxworth JE, Hawkes K. Ovarian follicle loss in humans and mice: lessons from statistical
609 model comparison. *Hum Reprod*. 2010;25(7):1796-1805. doi:10.1093/humrep/deq136
- 610 29. Best CL, Pudney J, Welch WR, Burger N, Hill JA. Localization and characterization of white
611 blood cell populations within the human ovary throughout the menstrual cycle and
612 menopause. *Hum Reprod*. 1996;11(4):790-797.
613 doi:10.1093/oxfordjournals.humrep.a019256
- 614 30. Pate JL. Involvement of immune cells in regulation of ovarian function. *J Reprod Fertil*
615 *Suppl*. 1995;49:365-377. doi:10.1530/biosciproc.3.028
- 616 31. Wu R, Van der Hoek KH, Ryan NK, Norman RJ, Robker RL. Macrophage contributions to
617 ovarian function. *Hum Reprod Update*. 2004;10(2):119-133. doi:10.1093/humupd/dmh011

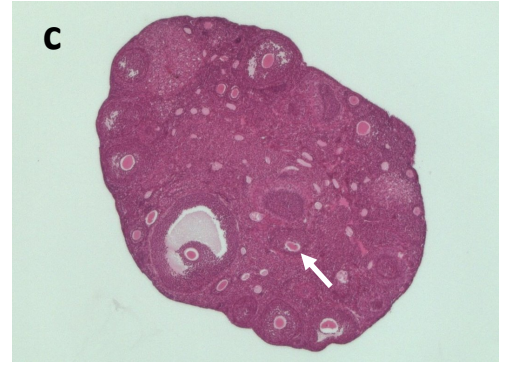
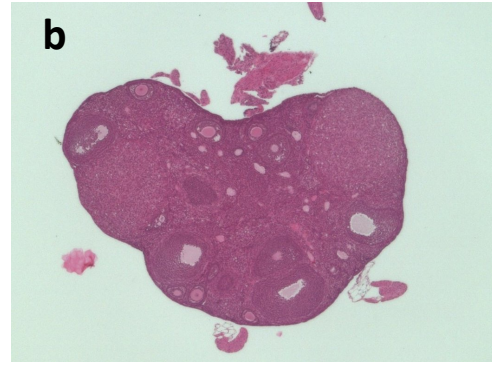
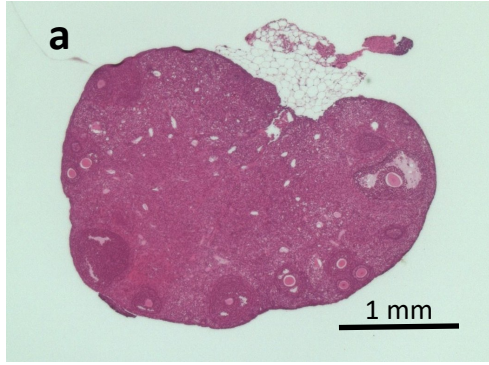
- 618 32. Sharif K, Watad A, Bridgewood C, Kanduc D, Amital H, Shoenfeld Y. Insights into the
619 autoimmune aspect of premature ovarian insufficiency. *Best Pract Res Clin Endocrinol*
620 *Metab.* 2019;33(6):101323. doi:<https://doi.org/10.1016/j.beem.2019.101323>
- 621 33. Zimon A, Erat A, Reindollar R, Usheva A. NFκB and other markers of chronic inflammation
622 in the prediction of ovarian aging and infertility. *Fertil Steril.* 2004;82(September):S318.
623 doi:[10.1016/j.fertnstert.2004.07.857](https://doi.org/10.1016/j.fertnstert.2004.07.857)
- 624 34. Lliberos C, Liew SH, Zareie P, La Gruta NL, Mansell A, Hutt K. Evaluation of inflammation
625 and follicle depletion during ovarian ageing in mice. *Sci Rep.* 2021;11(1):1-15.
626 doi:[10.1038/s41598-020-79488-4](https://doi.org/10.1038/s41598-020-79488-4)
- 627 35. Tuğrul Ayanoğlu B, Özdemir ED, Türkoğlu O, Alhan A. Diminished ovarian reserve in
628 patients with psoriasis. *Taiwan J Obstet Gynecol.* 2018;57(2):227-230.
629 doi:[10.1016/J.TJOG.2018.02.010](https://doi.org/10.1016/J.TJOG.2018.02.010)
- 630 36. Zhao Y, Chen B, He Y, et al. Risk Factors Associated with Impaired Ovarian Reserve in
631 Young Women of Reproductive Age with Crohn's Disease. *ir.* 2020;18(2):200-209.
632 doi:[10.5217/ir.2019.00103](https://doi.org/10.5217/ir.2019.00103)
- 633 37. Alesi LR, Winship AL, Hutt KJ. Evaluating the impacts of emerging cancer therapies on
634 ovarian function. *Curr Opin Endocr Metab Res.* 2021;18:15-28.
635 doi:[10.1016/j.coemr.2020.12.004](https://doi.org/10.1016/j.coemr.2020.12.004)
- 636 38. Cai L, Li Y, Tan J, Xu L, Li Y. Targeting LAG-3, TIM-3, and TIGIT for cancer
637 immunotherapy. *J Hematol Oncol.* 2023;16(1):1-34. doi:[10.1186/s13045-023-01499-1](https://doi.org/10.1186/s13045-023-01499-1)
- 638 39. Schmid P, Cortes J, Puztai L, et al. Pembrolizumab for Early Triple-Negative Breast
639 Cancer. *N Engl J Med.* 2020;382(9):810-821. doi:[10.1056/nejmoa1910549](https://doi.org/10.1056/nejmoa1910549)
- 640 40. Takahashi M, Cortés J, Dent R, et al. Pembrolizumab Plus Chemotherapy Followed by
641 Pembrolizumab in Patients With Early Triple-Negative Breast Cancer. *JAMA Netw Open.*
642 2023;6(11):e2342107. doi:[10.1001/jamanetworkopen.2023.42107](https://doi.org/10.1001/jamanetworkopen.2023.42107)
- 643 41. Kedem-Dickman A, Maman E, Yung Y, et al. Anti-Müllerian hormone is highly expressed
644 and secreted from cumulus granulosa cells of stimulated preovulatory immature and atretic
645 oocytes. *Reprod Biomed Online.* 2012;24(5):540-546. doi:[10.1016/j.rbmo.2012.01.023](https://doi.org/10.1016/j.rbmo.2012.01.023)

- 646 42. Saadia Z. Follicle Stimulating Hormone (LH: FSH) Ratio in Polycystic Ovary Syndrome
647 (PCOS) - Obese vs. Non- Obese Women. *Med Arch (Sarajevo, Bosnia Herzegovina)*.
648 2020;74(4):289-293. doi:10.5455/medarh.2020.74.289-293
- 649 43. Chaqour J, Ozcan MCH, De La Cruz P, Woodman-Sousa MF, McAdams JN, Grive KJ.
650 Effects of Maternal Taxane Chemotherapy Exposure on Daughters' Ovarian Reserve and
651 Fertility Potential. *F&S Sci*. Published online 2023. doi:10.1016/j.xfss.2023.10.003
- 652 44. Le Naour A, Koffi Y, Diab M, et al. EO771, the first luminal B mammary cancer cell line
653 from C57BL/6 mice. *Cancer Cell Int*. 2020;20(1):328. doi:10.1186/s12935-020-01418-1
- 654 45. Ueha S, Yokochi S, Ishiwata Y, et al. Robust antitumor effects of combined anti-CD4-
655 depleting antibody and anti-PD-1/PD-L1 immune checkpoint antibody treatment in mice.
656 *Cancer Immunol Res*. 2015;3(6):631-640. doi:10.1158/2326-6066.CIR-14-0190
- 657 46. Woodman MF, Ozcan MCH, Gura MA, De La Cruz P, Gadson AK, Grive KJ. The
658 requirement of ubiquitin C-terminal hydrolase L1 in mouse ovarian development and
659 fertility. *Biol Reprod*. Published online May 3, 2022:ioac086. doi:10.1093/biolre/ioac086
- 660

anti-PD-1

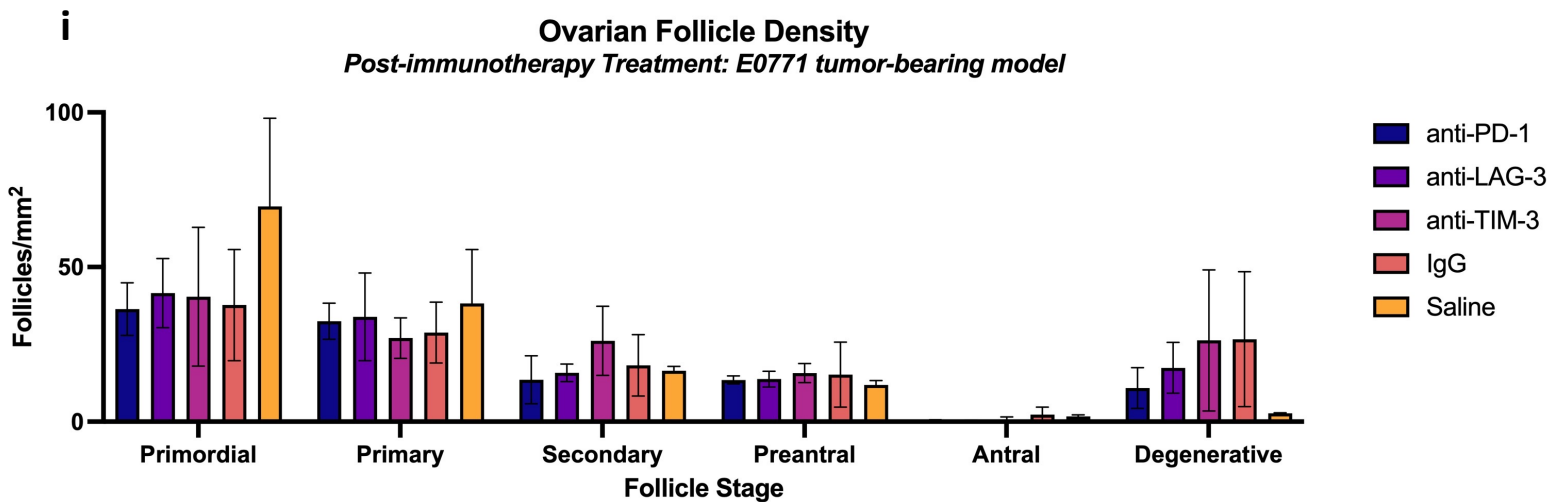
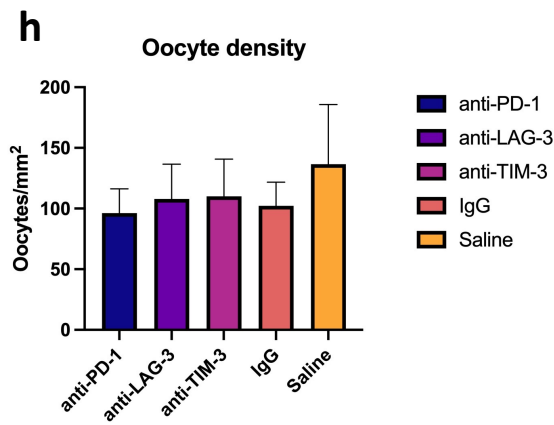
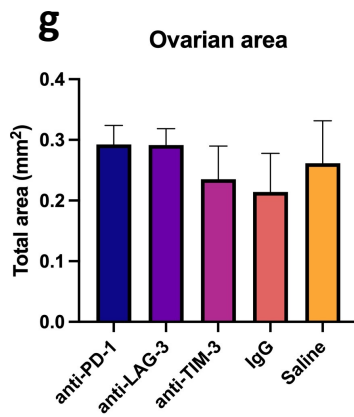
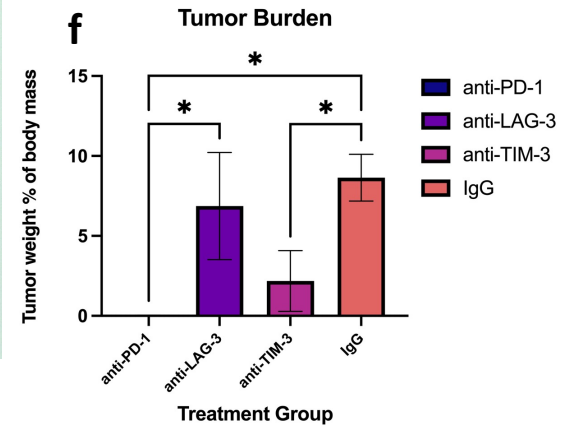
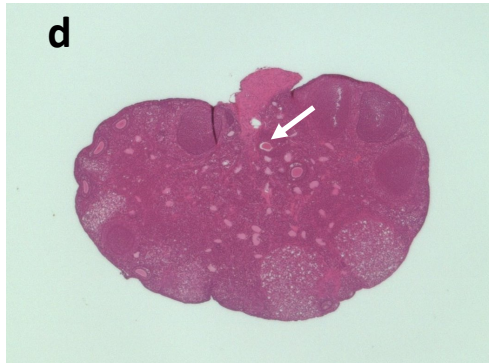
anti-LAG-3

anti-TIM-3



IgG isotype control

Healthy control (Saline mock-injected)



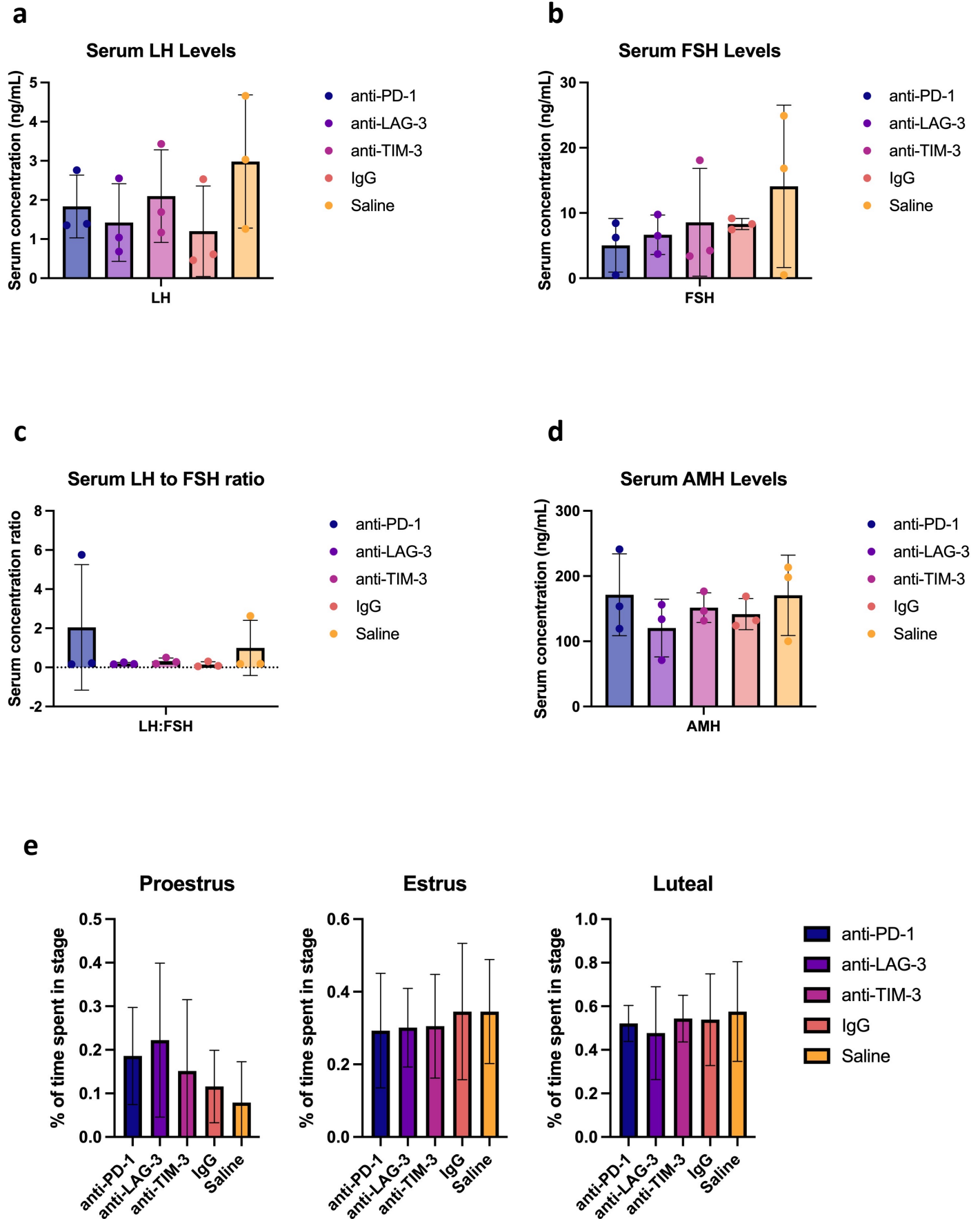


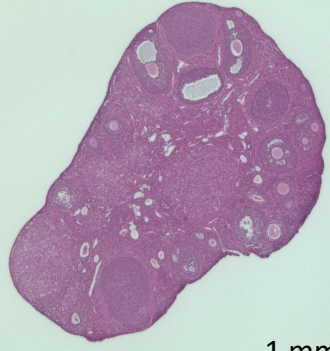
Figure 3

anti-PD-1

IgG isotype control

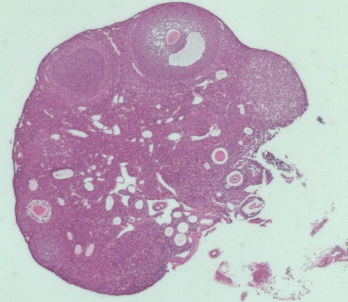
Saline control

a

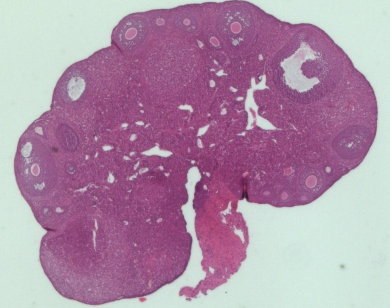


1 mm

b

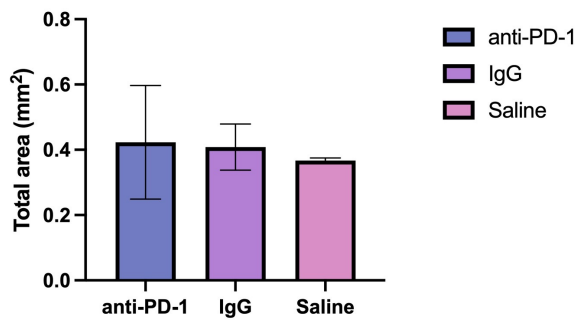


c



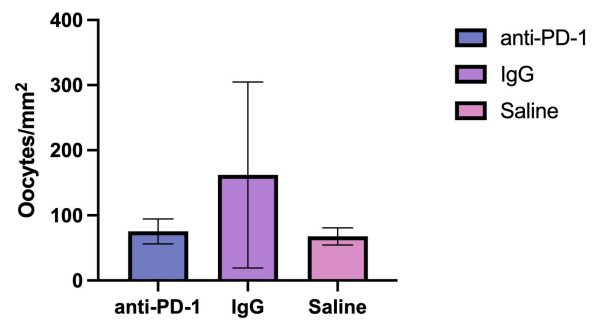
d

Ovarian area



e

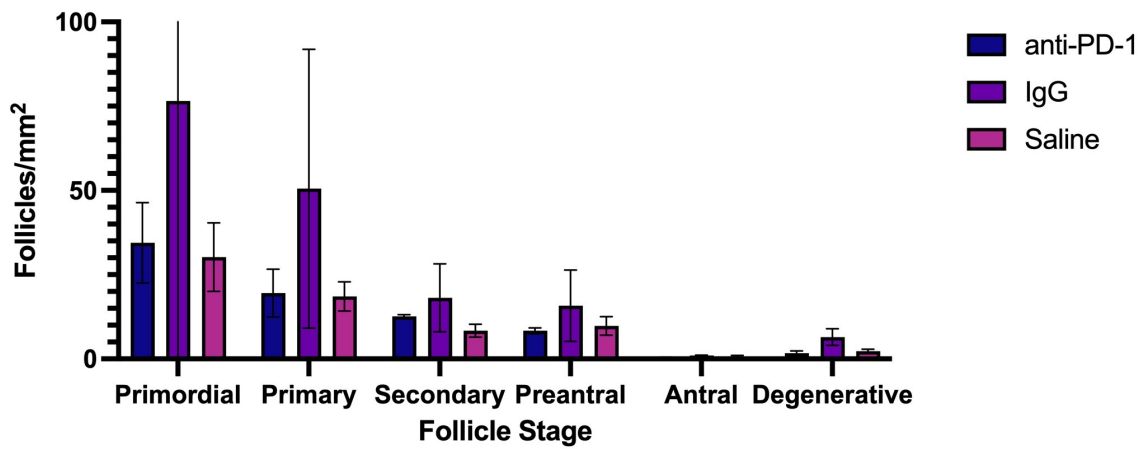
Oocyte density



f

Ovarian Follicle Density

Post-immunotherapy Treatment: Non-tumor-bearing model



g

Proestrus

Estrus

Luteal

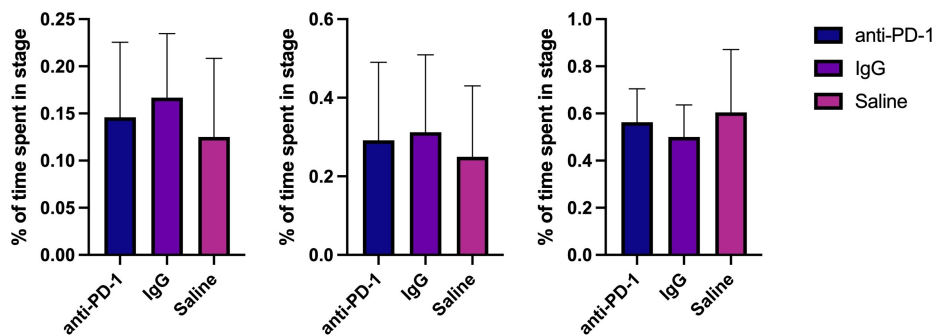
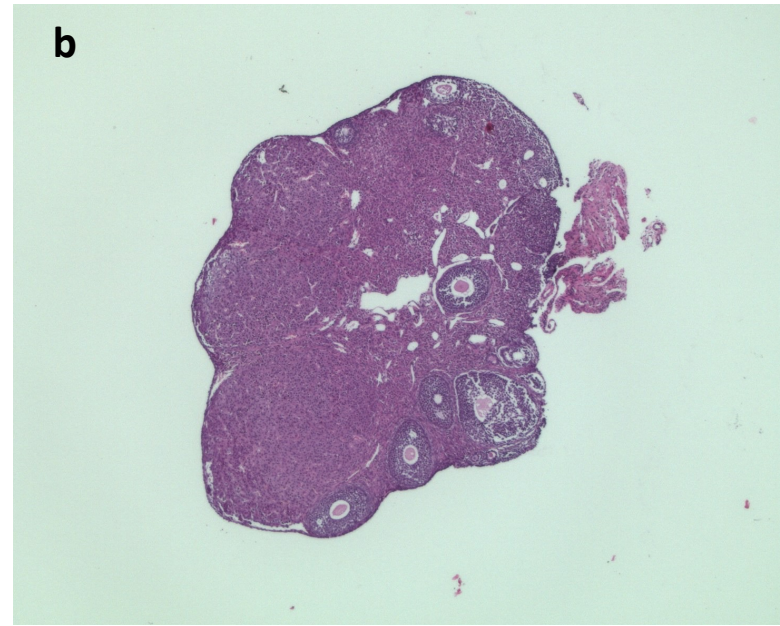
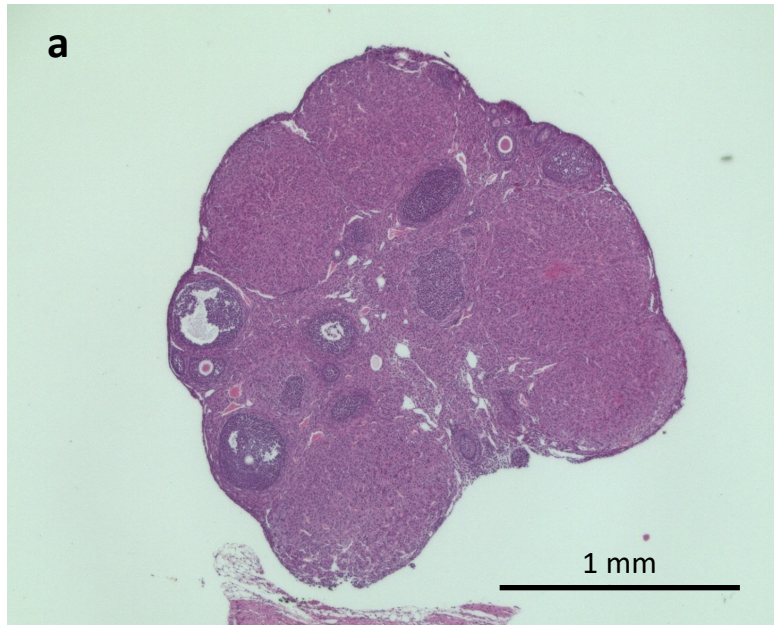


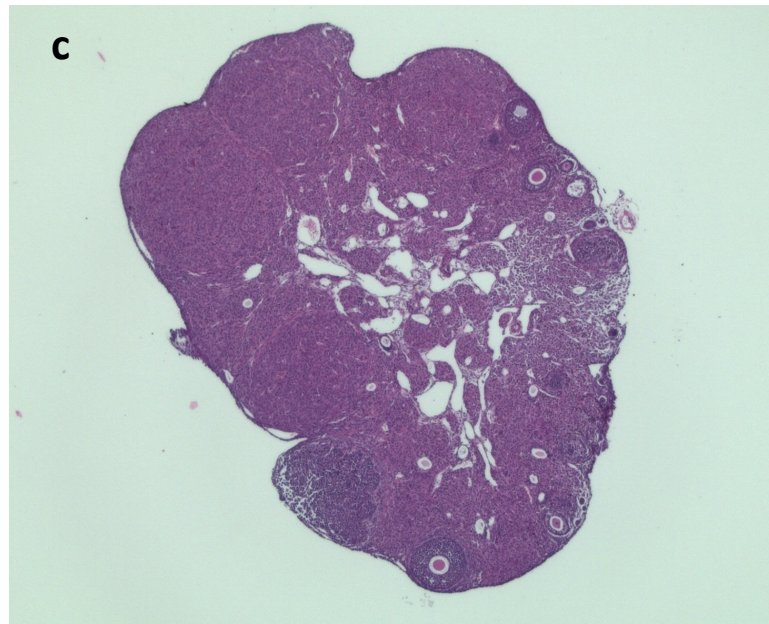
Figure 4

anti-PD-1

IgG isotype control

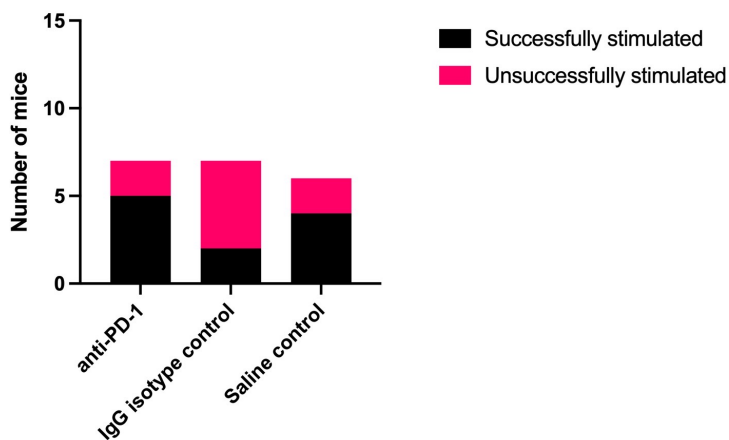


Saline control



d

Number of responders to hormonal stimulation



e

Retrieved oocytes per stimulated mouse

